

Implementation of TKE-Advection in COSMO 5.0 for `itype_turb=3`

Ulrich Blahak, DWD

May 6, 2014

Up to now the advection of TKE was only implemented for the alternative turbulence schemes from the LLM-project (`itype_turb=5...8`). It can be activated by by choosing `lprog_tke=.TRUE.` and is only possible when using the Runge-Kutta-Core. This process has now also been implemented for the “standard” scheme (`itype_turb=3`), still only for Runge-Kutta-dynamics.

Note that the switch `lprog_tke=.TRUE.` has a slightly different meaning in the different schemes. Whereas it only denotes the advection process for `itype_turb=3`, it also switches on the horizontal and vertical diffusion for the schemes `itype_turb=5...8`. The latter processes are active in `itype_turb=3` in any case.

The implementation is along the lines of the COSMO tracer advection schemes. Semi-lagrange advection, flux-form density-based advection (Bott et al.) or the traditional formulation with divergence correction can be used.

For `itype_turb=3`, the transported quantity is the turbulent velocity scale $q = \sqrt{2 \text{TKE}}$, but for `itype_turb=5...8` it is directly the TKE. For the flux-form density-based advection schemes, the transported quantities are multiplied with the total density before the advection operator — to transform them to densities for the advection operator — and divided by the advected density afterwards, same as for the tracers. Because TKE is defined on half levels, the density values to multiply with have to be vertically interpolated to the half levels, which is done by linear interpolation. The same applies for the advected density to be divided by afterwards.

Technically, the advection is done slightly differently for the different turbulence schemes:

- `itype_turb=3`: The advective tendency $\text{TEND}_{adv} = (q_{after} - q_{before})/\Delta t$ is stored on a new global field `tket_adv(1:ie,1:je,1:ke)` and added to q in the call to the subroutine `turbdiff()` in the next timestep, together with the other physical tendencies of q .
- `itype_turb=5...8`: “update in place” of the advected quantity on timelevel `nnew`

A slight complication arises for `itype_turb=3` because of the exponential filtering of q to damp numerical local oscillations during time integration. The relevant namelist parameter is `tkesmot`, which is the weight a in the recursive exponential time filter

$$q_{n+1} = (1 - a)q_{n+1}^* + aq_n \quad (1)$$

where q_n is the “old” value, q_{n+1} the “new” and q_{n+1}^* is the result of an implicit time integration step,

$$q_{n+1}^* = \text{fct} (q_n, q_{n+1}^*, \text{TEND}(q_n), \Delta t) \quad (2)$$

It is obvious that, if we would include the advection in the total tendency $\text{TEND}(q_n)$, the transport velocity of TKE structures would be reduced by the factor a , which is physically wrong. To mitigate this problem and at the same time to keep the possibility for time smoothing, the procedure is modified. In a first explicit Euler-Forward-step, only the advective tendency $\text{TEND}_{adv}(q_n)$ is applied to obtain a provisional value q_{n+1}^{**} ,

$$q_{n+1}^{**} = q_n + \text{TEND}_{adv}(q_n)\Delta t \quad (3)$$

Then, the implicit scheme is applied to this provisional value, neglecting the advective tendency,

$$q_{n+1}^* = \text{fct} (q_{n+1}^{**}, q_{n+1}^*, \text{TEND}(q_n) - \text{TEND}_{adv}(q_n), \Delta t) \quad (4)$$

followed by the time filtering

$$q_{n+1} = (1 - a)q_{n+1}^* + aq_n^* \quad (5)$$

In this way, the time filtering is only applied to the non-advective part of the TKE-changes.

Note that, for the diffusion process of TKE, there is a similar problem with the spatial propagation speed of the diffusion signal, and in the future, the diffusion tendency should also somehow be removed from the time filtering.

As a first testing step, a simple 2D idealized test case (flow over hill) has been set up. A cuboid package of high TKE values ($50 \text{ m}^2\text{s}^{-2}$) is artificially introduced near the inflow boundary of the domain, and the output is analyzed every timestep. The spatial resolution was $\Delta X = 1.1 \text{ km}$, the time step $\Delta T = 10 \text{ s}$ and 40 vertical levels up to 22 km height have been chosen. The initial wind speed is a constant $U = 10 \text{ ms}^{-1}$ everywhere (no lateral and vertical motion) and the temperature decreases linearly with height at the ICAO standard atmosphere gradient. With that, we have a stable stratification and very low windshear and expect pure horizontal transport.

This setup has been run for both `itype_turb=3` and `itype_turb=7` to test the two above-mentioned different implementations of TKE advection. Fig. 1 to 4 show the results for both runs for different simulation times, starting with the initial state (Fig. 1) and ending with 15 min (Fig. 4). Slight differences in the initial state are due to the fact that the output of TKE in the first timestep includes or excludes the time-changes during the first time step. For `itype_turb=7`, the output is on timelevel “nnow” as for the other prognostic model variables, so no changes occurred. But in case of `itype_turb=3`, the local changes due to some TKE sources and sinks (not the advection and diffusion and possibly some others!) have already been added in the first time step.

One can see that in both cases the TKE-cuboid is transported with about the same speed, but there are differences in the vertical. Therefore, the advection is implemented properly and happens at the expected speed. We expect no advection errors in the other transport directions, because the same well-tested subroutines as for the tracers are applied in the same way.

However, the vertical differences require some more consideration. It turns out that these are due to differences in the turbulent diffusion of TKE. Note that the values of the Richardson

Number $Ri = N^2/S^2$ ($N =$ Brunt-Visla frequency, $S =$ total shear) are quite high, so that in reality, we expect the TKE to die out very soon, associated with low turbulent mixing. This “stable” case is treated differently in both turbulence schemes. For `itype_turb=7`, the diffusion coefficients are simply set to a low value ($0.1 \text{ m}^2\text{s}^{-1}$) regardless of the TKE, whereas they are still a function of stability and TKE in case of `itype_turb=3`. This explains why the blob of spuriously high TKE is strongly diffused in the latter case and nearly not diffused in the former.

The use of the already existing namelist parameter `lprog_tke` to switch on the advection of TKE for `itype_turb=3` requires some clarification, because its meaning is slightly different in case of the alternative schemes `itype_turb=7` and `8`. And in combination with the parameter `l3dturb` (“3D-turbulence”), different terms of the TKE-equation are actually considered. Tab. 1 summarizes these considered terms for `itype_turb=3` and Tab. 2 for `itype_turb=7` and `8`.

For `itype_turb=3`, the activation of `lprog_tke` has been tested by a real case COSMO_DE hindcast of 31.5.2011, 12 UTC +21 h, driven by the operational COSMO_DE-analyses (`l3dturb` remained `.false.`). Two model runs were performed, one with `lprog_tke=.false.` and the other with `.true.`. The 3D-turbulence was deactivated, consistent with the operational setup of COSMO_DE. The only difference between the two runs is thus the consideration of TKE-Advection (cf. Tab. 1, first and third column). Fig. 5 shows T_{2M} (upper row) and accumulated total precipitation (lower row) after 21 h at the end of the forecast. The left column is without TKE-Advection, the middle column with TKE-Advection and the right column is the difference with minus without. No significant differences for the T_{2M} can be observed, only a wave-like pattern, perhaps indicating spatial shifts, is visible in the difference plot. This is generally similar also for the total precipitation, except for a region south of the Erzgebirge, Eastern Bavaria and Western Czechia. Here, the consideration of the TKE-Advection shifted the precipitation pattern a little to the South.

However, for both quantities, the domain averaged systematic difference is very very small. The effect of considering the TKE-Advection has therefore no significant effect on the weather forecast in this case. However, this has to be checked by a longer term experiment.

To further illustrate the effects of the different switches/processes in Tab. 1 and Tab. 2 on very high resolution runs, a series of idealized LES-like simulations with a horizontal grid spacing of $\Delta X = 200 \text{ m}$ has been performed. The runs are characterized by 125×125 grid points in the horizontal, 64 levels in the vertical up to 15 km height, periodic boundary conditions, flat terrain, condensation and cloud microphysics switched off, soil model switched off, radiation switched off, deep and shallow convection parameterization switched off, usage of the new fast waves solver in the Runge-Kutta core, and a forced constant sensible heat flux of $H_0 = 300 \text{ Wm}^{-2}$ at the surface. The initial T -profile in the PBL is slightly stable with a T lapse rate of $\approx -0.007 \text{ Km}^{-1}$, and the wind profile is $U(z) = U_\infty \tanh(z/z_{ref})$ with $U_\infty = 5 \text{ ms}^{-1}$ and $z_{ref} = 3000 \text{ m}$. Some small random noise on T and w is added at simulation start in the lowest 100 hPa of the atmosphere to initiate motions on different scales from which shallow convection will spin up later.

For each of the 4 possible combinations of the switches `lprog_tke` and `l3dturb` and each of `itype_turb=3` and `7`, a model run has been performed out to +4 h. Fig. 6 shows horizontal cross sections of w at a height of about 700 m after 4 h for each of the 4 switch combinations in case of `itype_turb=3`. Fig. 7 is the same, but for `itype_turb=7`. From convection theory and measurements, one would expect to see coherent and organized up- and downdraft

structures with a more cellular pattern close to the ground and more isolated updrafts above (“Thermals”), growing from the cell corners with converging horizontal motions. The updraft regions should be smaller than the downdraft regions, and the maximum updrafts “stronger” than the maximum downdrafts, but not more than, say, $5 - 6 \text{ ms}^{-1}$. The diameter of the cellular patterns respectively the average distance between the thermals should scale with the boundary layer height and be about 2 - 5 times this height.

With this in mind, an inspection of Fig. 6 for `itype_turb=3` shows clearly that without 3D turbulence effects (upper row), the coherent structures are strongly overlaid by spurious noise, which turn out to be $2\Delta x$ waves caused by spurious energy accumulation at the smallest grid scales (“under-diffusive” turbulence scheme). Setting `l3dturb=.true.` completely changes the picture (lower row). The added horizontal diffusion effects (cf. Tab. 1) cause a very strong smoothing of the structures, eliminating any $2\Delta x$ waves. The w structures seem qualitatively realistic, although in the opinion of the author somewhat overly smooth. A closer look at power spectra could shed more light on this in the future. Adding the horizontal shear production

Table 1: `itype_turb=3`: Considered processes in the *TKE*-equation for the different combinations of `lprog_tke` and `l3dturb`.

<code>lprog_tke</code>	<code>.false.</code>	<code>.false.</code>	<code>.true.</code>	<code>.true.</code>
<code>l3dturb</code>	<code>.false.</code>	<code>.true.</code>	<code>.false.</code>	<code>.true.</code>
∂_t	X	X	X	X
Therm. prod.	X	X	X	X
Horiz. Shear prod.		X		X
Vert. Shear prod.	X	X	X	X
Dissipation	X	X	X	X
Horiz. diffus.				X
Vert. diffus	X	X	X	X
Advection			X	X

Table 2: Same as Tab. 1, but for `itype_turb=7` and `8`.

<code>lprog_tke</code>	<code>.false.</code>	<code>.false.</code>	<code>.true.</code>	<code>.true.</code>
<code>l3dturb</code>	<code>.false.</code>	<code>.true.</code>	<code>.false.</code>	<code>.true.</code>
∂_t			X	X
Therm. prod.	X	X	X	X
Horiz. Shear prod.		X		X
Vert. Shear prod.	X	X	X	X
Dissipation	X	X	X	X
Horiz. diffus.				X
Vert. diffus			X	X
Advection			X	X

(by setting `l3dturb=.true.`) has the biggest impact, whereas adding *TKE*-advection (by setting `lprog_tke=.true.`) does not change the results much (maybe because of the quite low windspeed).

The situation in Fig. 7 for `itype_turb=7` is slightly different. The $2\Delta x$ waves vanish here when setting `lprog_tke=.true.` and `l3dturb=.true.` (lower right panel). Then, the w structures look very realistic (considering the relatively coarse grid resolution for this phenomenon) and are not overly smoothed. The author considers this as the “best” simulation of the series.

Concerning the different behaviour of the two turbulence schemes, the meaning of the two switches `l3dturb` and `lprog_tke` is different among the two turbulence schemes, see Tables 1 and 2. Whereas for `itype_turb=3`, `lprog_tke` concerns only the *TKE*-advection and the *TKE* horizontal diffusion in case of `l3dturb=.true.`, it is connected to the prognostic treatment of *TKE* and to its advection and diffusion for `itype_turb=7`.

From the different behaviour visible in Figures 6 and 7, one possible conclusion is that mainly the consideration of the horizontal shear production in combination with *TKE* diffusion (vertical, horizontal) enhances the quality of the results in the presented case.

The different “degree of smoothing” of the w structures, perhaps associated with a different behaviour of the power spectra, might be explained by the different approaches to parameterize the turbulent length scale in the two turbulence schemes.

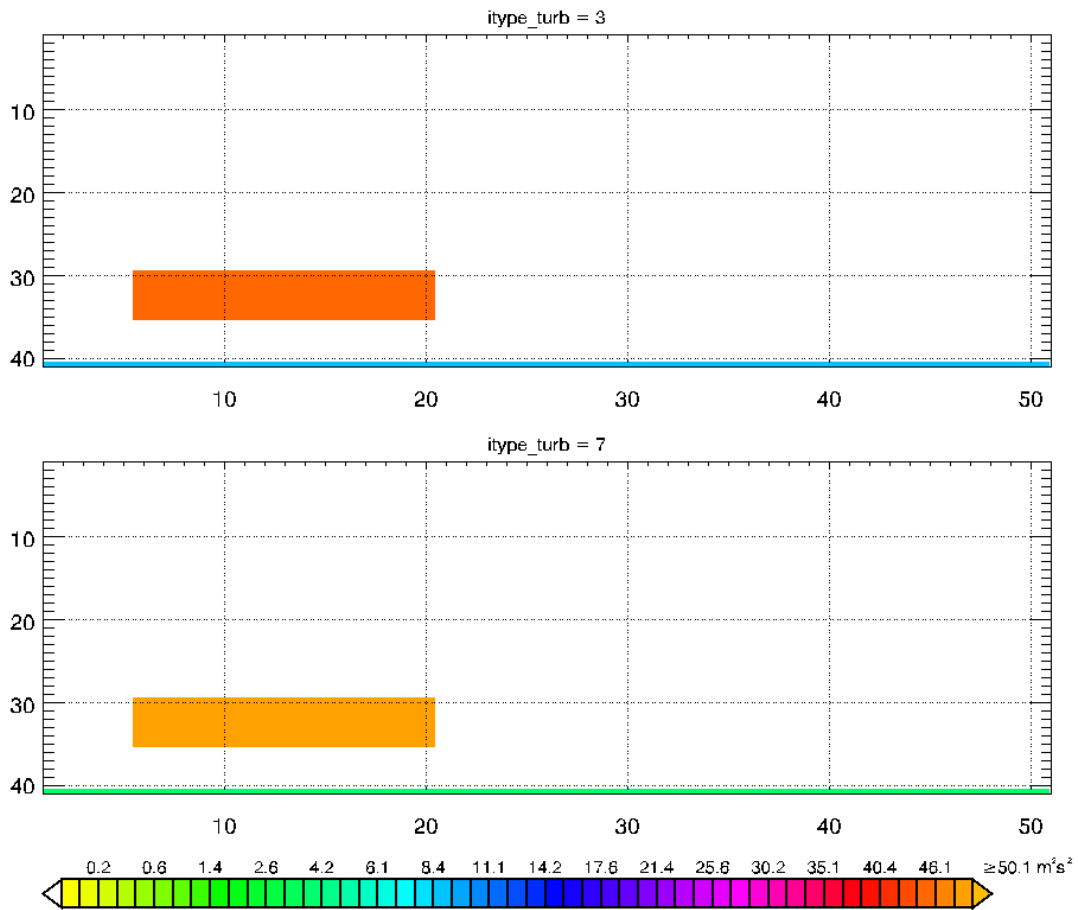


Figure 1: Simple test of the TKE advection for `itype_turb=3` and `7`. X - Z -cut along the 2D flow, $U = 10 \text{ ms}^{-1}$ everywhere from left to right, stable stratification (ICAO-standard atmosphere). Initial values for the TKE.

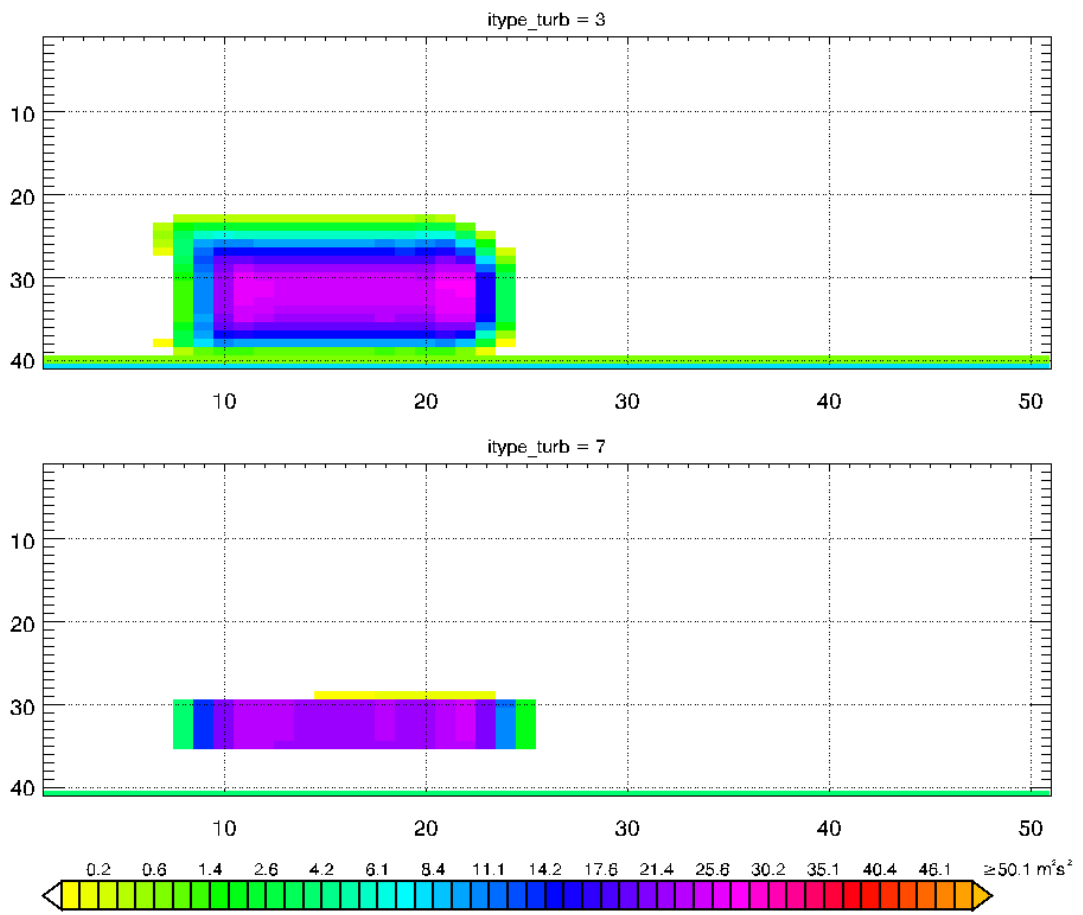


Figure 2: Same as Fig. 1 but after 2 minutes.

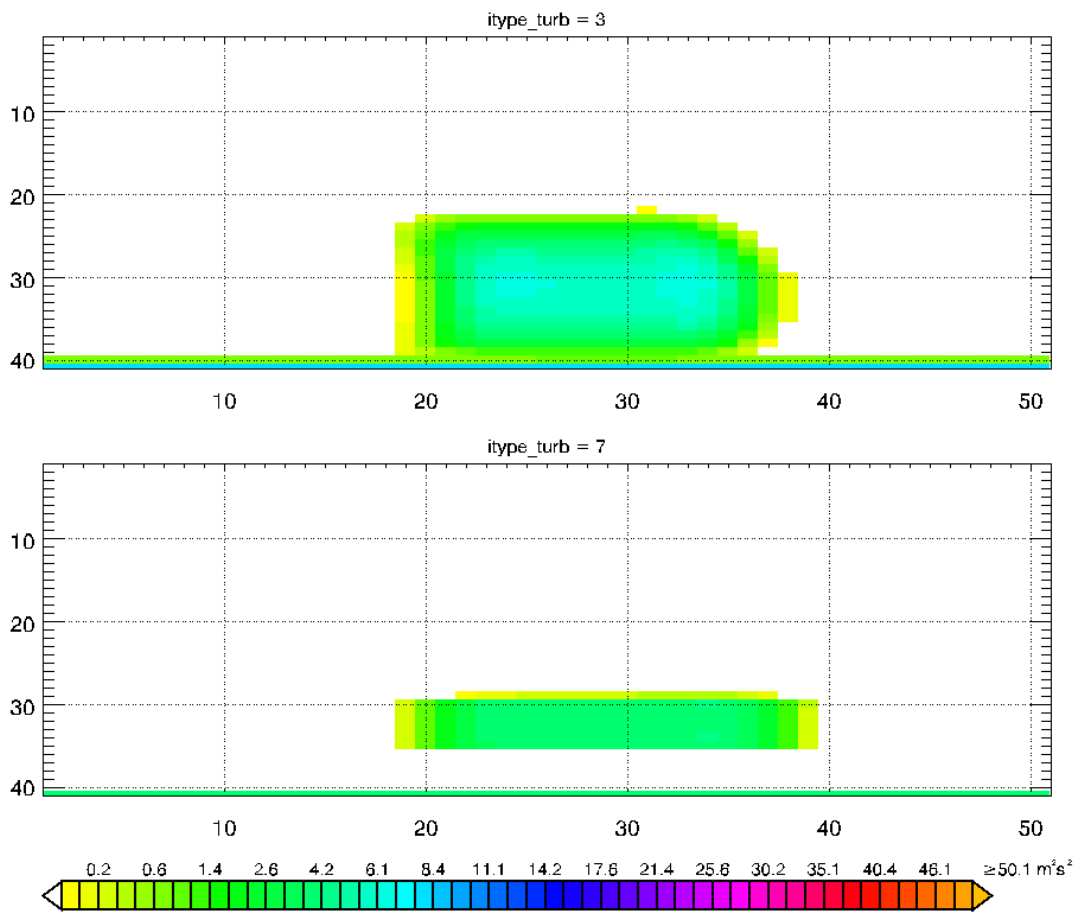


Figure 3: Same as Fig. 1 but after 10 minutes.

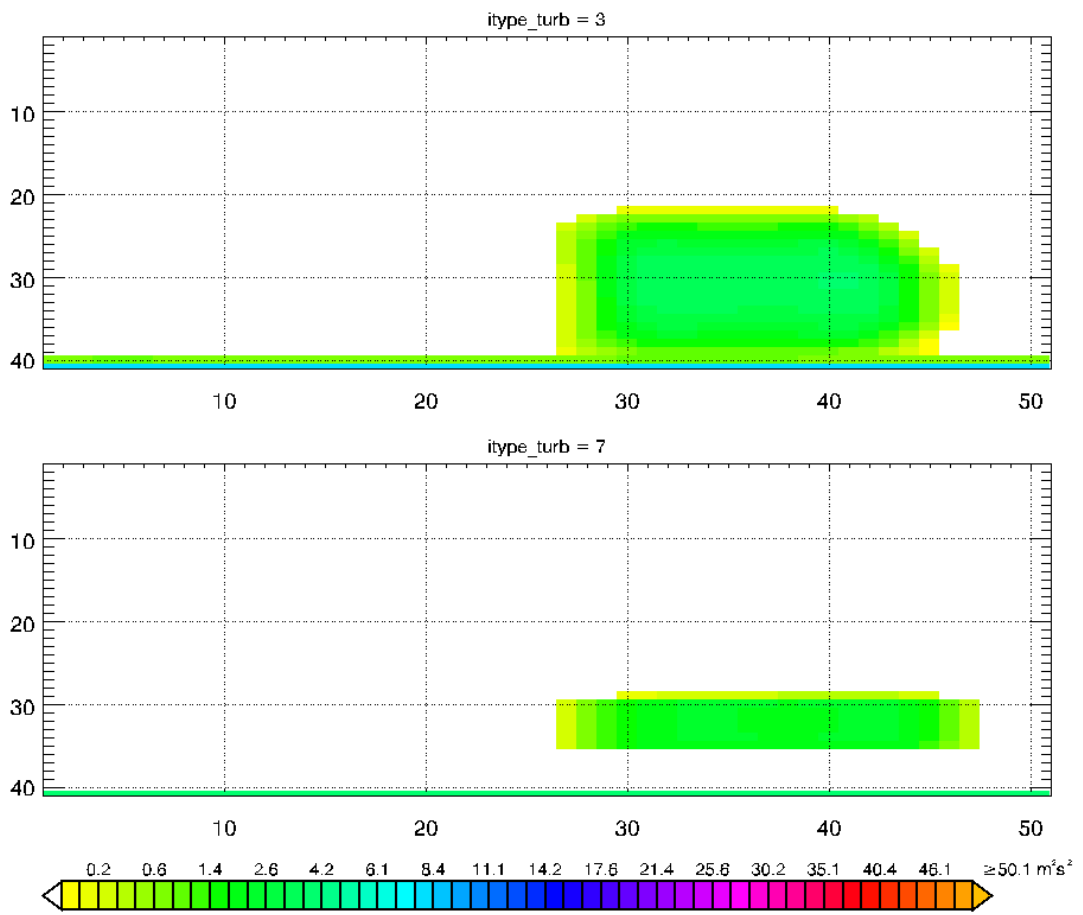


Figure 4: Same as Fig. 1 but after 15 minutes.

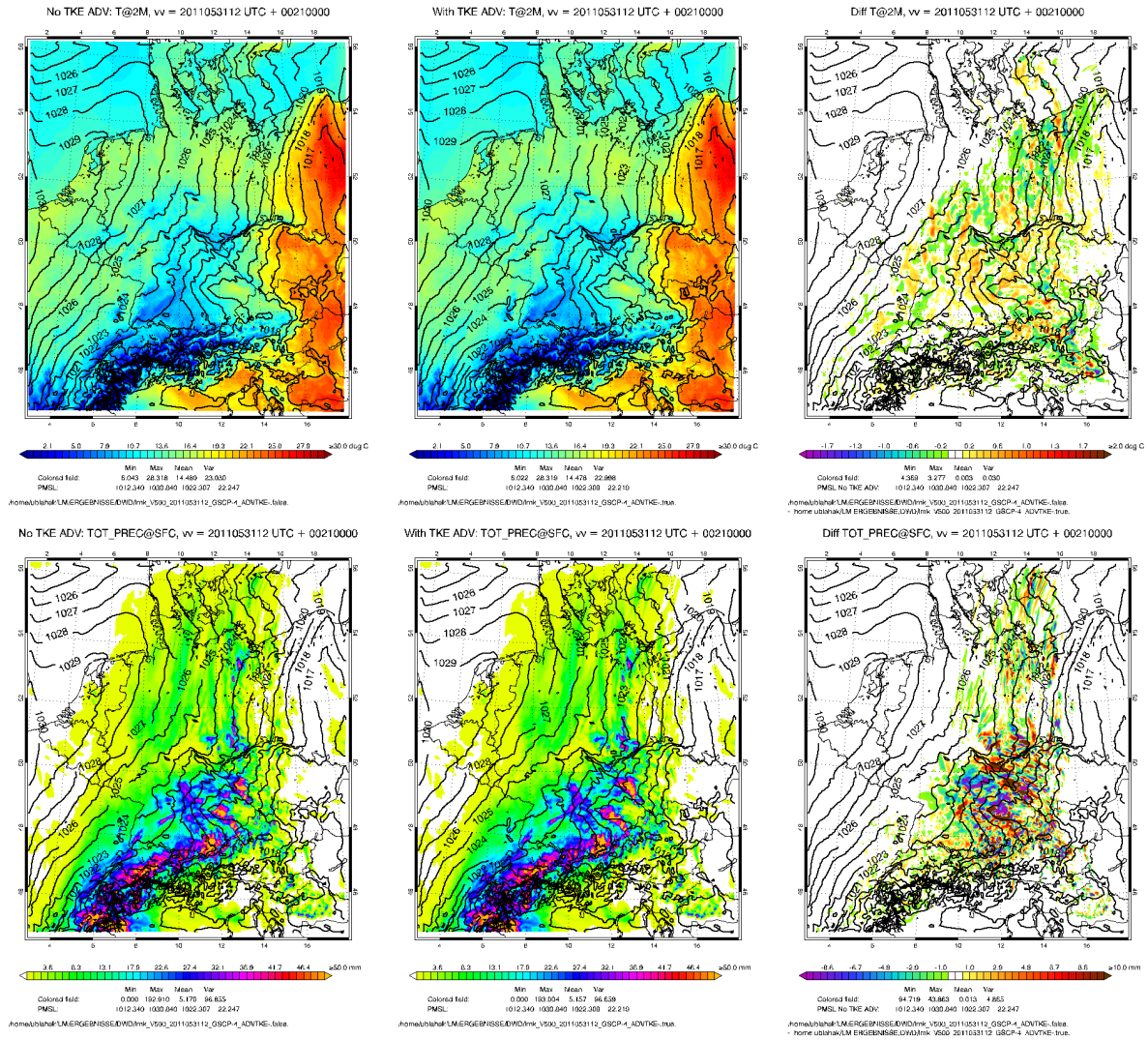


Figure 5: COSMO_DE hindcast, 31.5.2011 12 UTC + 21 h, $i_{\text{type_turb}}=3$. **Upper left:** T_{2m} , no TKE advection. **Upper middle:** T_{2m} , TKE advection. **Upper right:** Difference middle to left. **Lower left:** Total precip, no TKE advection. **Lower middle:** Total precip, TKE advection. **Lower right:** Difference middle to left.

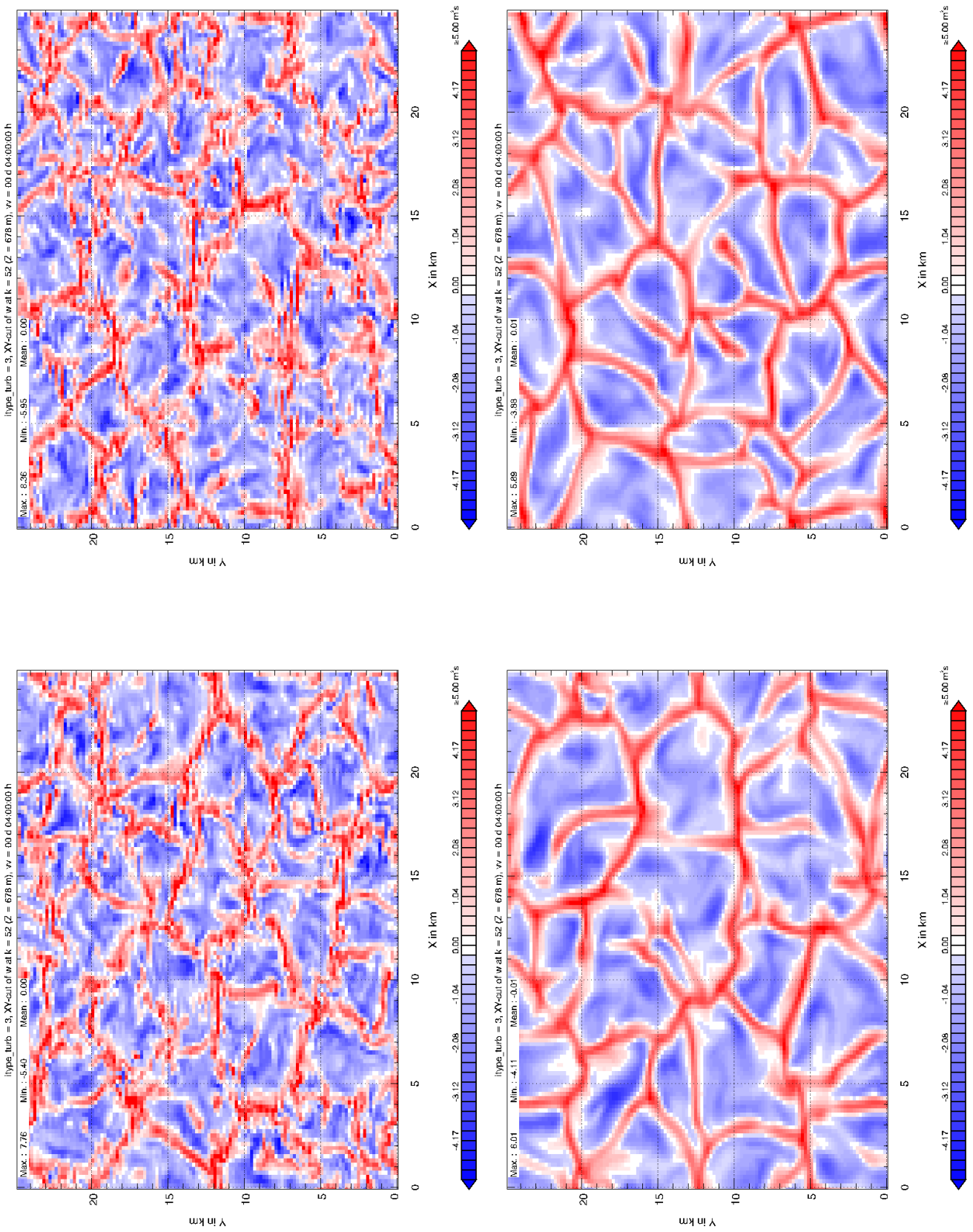


Figure 6: LES experiment: $H_0 = 300 \text{ W m}^{-2}$, $\Delta X = 200 \text{ m}$, 4 h after simulation start, `ltype_turb=3, l3dturb=.false., l3dturb=.true., l3dturb=.true..` **Upper left:** `lprog_tke=.false., l3dturb=.false..` **Upper right:** `lprog_tke=.true., l3dturb=.false., l3dturb=.true..` **Lower left:** `lprog_tke=.false., l3dturb=.false., l3dturb=.true..` **Lower right:** `lprog_tke=.true., l3dturb=.true..`

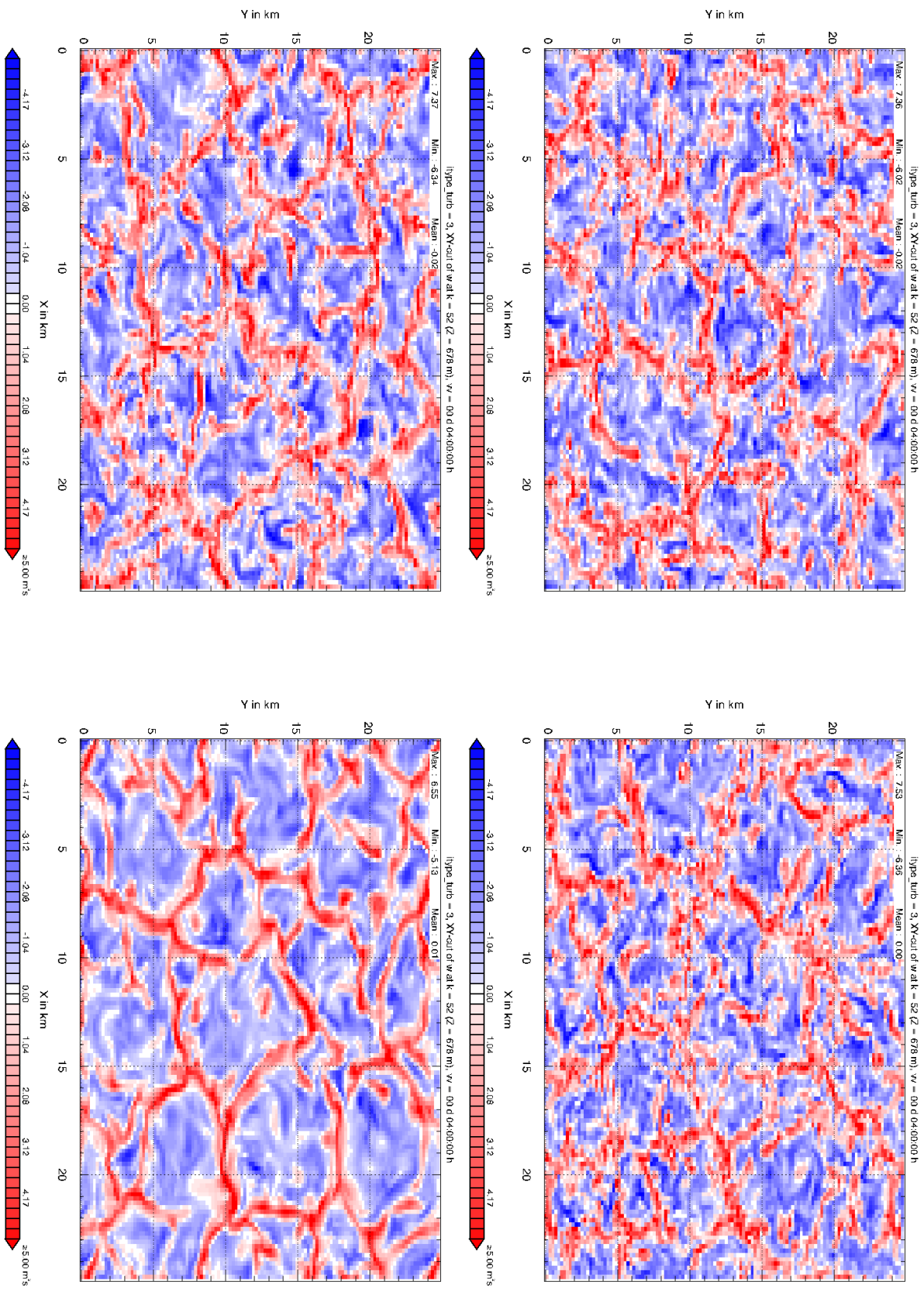


Figure 7: LES experiment: $H_0 = 300 \text{ Wm}^{-2}$, $\Delta X = 200 \text{ m}$, 4 h after simulation start, `itype_turb=7`. **Upper right:** `l3dturb=.false., l3dturb=.false.` **Upper right:** `l3dturb=.true., l3dturb=.false.` **Lower left:** `l3dturb=.false., l3dtk=7.` **Lower right:** `l3dturb=.true., l3dtk=7.`